Article

Mechanistic Insights into the Origin of Stereoselectivity in an Asymmetric Chlorolactonization Catalyzed by (DHQD)PHAL

Roozbeh Yousefi, Aritra Sarkar, Kumar Ashtekar, Daniel C. Whitehead, Tayeb Kakeshpour, Daniel Holmes, Paul Reed, James E. Jackson, and Babak Borhan

J. Am. Chem. Soc., **Just Accepted Manuscript** • DOI: 10.1021/jacs.0c01830 • Publication Date (Web): 21 Mar 2020

Mechanistic Insights into the Origin of Stereoselectivity in an Asymmetric Chlorolactonization Catalyzed by $(DHQD)_2PHAL$

Roozbeh Yousefi,[†] Aritra Sarkar,[†] Kumar Dilip Ashtekar,[†] Daniel C. Whitehead,[‡] Tayeb Kakeshpour, Daniel Holmes, Paul Reed, James E. Jackson* and Babak Borhan*

Department of Chemistry, Michigan State University, East Lansing, Michigan, 48824, United States

KEYWORDS (Word Style "BG_Keywords"). If you are submitting your paper to a journal that requires keywords, provide significant keywords to aid the reader in literature retrieval.

ABSTRACT: Electrophilic halofunctionalization reactions have undergone a resurgence sparked by recent discoveries in the field of catalytic asymmetric halocyclizations. To build mechanistic understanding of these asymmetric transformations, a toolbox of analytical methods has been deployed, addressing the roles of catalyst, electrophile (halenium donor), and nucleophile in determining rates and stereopreferences. The test reaction, $(DHQD)_2PHAL$-catalyzed chlorocyclization of 4-aryl-4-pentenoic acids with 1,3-dichloro-5,5-dimethylhydantoin (DCDMH), is revealed to be first order in catalyst and chlorenium ion donor and zero order in alkenoic acid substrate under synthetically relevant conditions. The simplest interpretation is that rapid substrate-catalyst binding precedes rate-limiting chlorenium attack, controlling the face selectivity of both chlorine attack and lactone closure. ROESY and DFT studies, aided by crystal structures of carboxylic acids bound by the catalyst, point to a plausible resting state of the catalyst-substrate complex predisposed for asymmetric chlorolactonization,. As revealed by our earlier labeling studies, these findings suggest modes of binding in the $(DHQD)_2PHAL$ chiral pocket that explain the system's remarkable control over rate- and enantioselection-determining events. Though a comprehensive modeling analysis is beyond the scope of the present work, quantum chemical analysis of the fragments' interactions and candidate reaction paths point to a one-step concerted process with the nucleophile playing a critical role in activating the olefin for concomitant electrophilic attack.

Introduction

Electrophilic olefin halocyclizations (Figure 1a) are long-known workhorse organic transformations,[1] now returning to prominence as their catalytic asymmetric variants offer a powerful strategy for enlarging the chiral pool.[2-50] In early work on 4-aryl-4-pentenoic acids, we found Sharpless's ligand, $(DHQD)_2PHAL$, to be an efficient mediator for asymmetric chlorolactonization (Figure 1b).[40,51] Since then, reports from our own and other labs have confirmed the efficacy of cinchona alkaloid dimers in a range of asymmetric halofunctionalizations.[17,19,22,41-43,52-55] With the growing list of examples, mechanistic insight into the catalytic activation and stereoinduction in these processes is necessary to support the design of new reactions and catalyst scaffolds. Taking $(DHQD)_2PHAL$-catalyzed asymmetric chlorolactonization of 4-aryl-4-propenoic acid as a test reaction, we present here kinetic, spectroscopic, structural, and computational studies leading to a mechanistic model.

Our recent labeling and spectroscopic analyses[56-57] revealed the absolute and relative face selectivities of Cl (electrophile) and O (nucleophile) addition across the double bond in **1** (Figure 1c) as well as the rate and stereochemical effects of varying the chlorohydantoins (chlorenium ion donors).[56-57] The cumulative findings of this work led to the following conclusions:

1. Catalyst templated addition across the olefin **1** shows both a strong pro-*R* preference (>20:1) for chlorenium ion attachment at C-6, and closure favoring the 5*R* over the 5*S* lactone by a factor of >10:1. The net result is predominant *syn* Cl, O addition across the olefinic π-bond in **1**-**D**, obviating the potential intermediacy of a 3-membered cyclic chloronium ion (Figure 1c).
2. In principle, the two new bonds in the major product stereoisomer **2**-**D** could be formed stepwise, *via* a carbocation intermediate, or concertedly (Figure 1c).
3. In either mechanistic case, the catalyst templates the ring closure. Catalyst binding, mainly *via* hydrogen bonding and van der Waals interactions, presumably limits the conformational choices of substrate **1**, guiding the enantioselective cyclization.
4. As depicted in Figure 2, we have probed the effects of tuning the chlorenium source in our asymmetric chlorolactonization protocol. By preparing and studying a series of previously unknown *N*-aroylated *N*-chlorohydantoins, we have shown that *N*1 substituents inductively activate delivery of the *N*3 chlorine to the substrate during the course of the chlorolactonization. The reaction rates of these electronically perturbed chlorinating agents vary as predicted by their *HalA* values (halenium affinity).[58] The linearity and low slope of the $\Delta\Delta G^{\ddagger}$ $[=RT\ln(k_{Ar}/k_{Ph})]$ vs *HalA* plot suggests an early transition state for chlorine transfer. Furthermore, chiral chlorohydantoins in these reactions display classic match-mismatch behaviors.[57] These results indicate direct involvement of the

chlorohydantoins in the rate and stereoselectivity-determining events in the asymmetric chlorocyclization.

These preliminary mechanistic findings call for a full investigation of the reaction mechanism to identify the modes of interaction among the participants, and to map out the catalytic cycle of this $(DHQD)_2PHAL$ catalyzed asymmetric chlorolactonization.

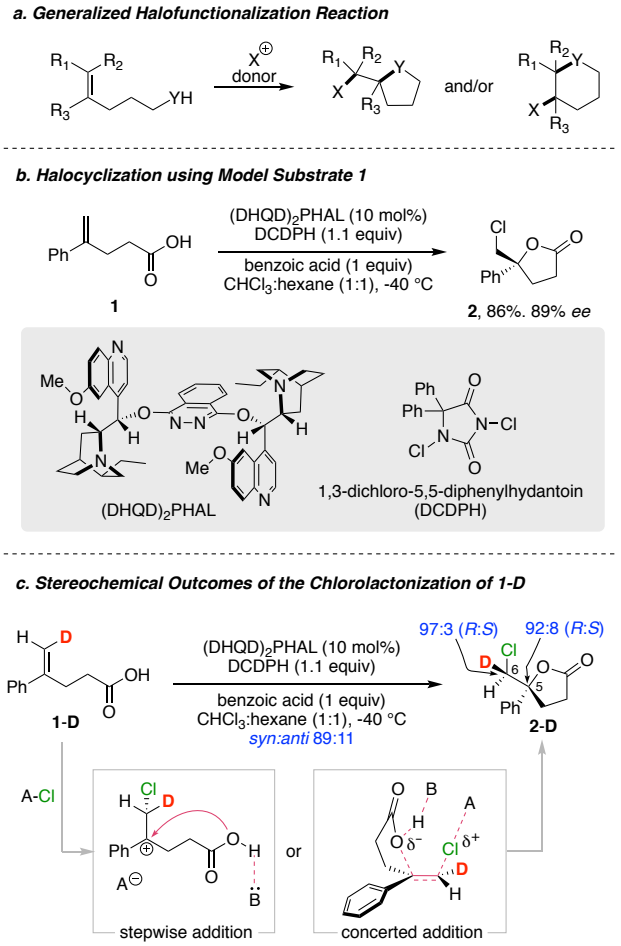

Figure 1. a. Generalized depiction of halocyclization reactions; b. Catalytic asymmetric chlorolactonization of 4-aryl-4-pentenoic acid **1** mediated by $(DHQD)_2PHAL$; c. Summary of observed stereoselectivities with deuterated substrate analog **1-D**, highlighting the *syn* addition as the major product of the catalytic reaction.

Results and Discussion

1. Kinetic Studies

Kinetic investigation of multistep organic reactions can provide key insights into reaction mechanisms by revealing the order of individual components in the rate-determining step (RDS). As articulated in recent years by Blackmond and co-workers,[59-62] Reaction Progress Kinetic Analysis (RPKA) exploits modern reaction monitoring methods and easily accessible fitting and graphing software to improve the ease and accuracy of analyses over classical approximation methods. A great advantage of RPKA is that it can probe practical reactions such as halofunctionalization under their native conditions, unlike classical kinetic treatments that require e.g. the unbalanced concentrations used in pseudo first order studies. In this work, RPKA results place critical boundary conditions on the mechanisms proposed for this asymmetric chlorolactonization.

In the original optimized reaction, 4-phenyl-4-pentenoic acid **1** at 0.051 M concentration was cyclized in the presence of 0.056 M 1,3-dichloro-5,5-diphenylhydantoin (DCDPH) as the chlorine source, along with 10 mol% $(DHQD)_2PHAL$ as the chiral catalyst. The highest enantioinduction was observed in a 1:1 chloroform:hexane mixture as solvent with benzoic acid as an additive at 0.051 M (Figure 1b).[40]

To follow the kinetics of this reaction, NMR analysis proved optimal as the reagent and products displayed well-resolved peaks under the reaction conditions. The following modifications to the standard protocol were introduced to simplify the mixture for kinetic studies: (i) deuterated chloroform was employed instead of 1:1 chloroform:hexane; (ii) 4 mol% of the catalyst was used to slow the reaction, enabling capture of the important early data points. This approach allowed time for temperature equilibration in the probe and shimming, while retaining ≥85% of the starting material at the initial point of measurement; (iii) 1,3-dichloro-5,5-dimethylhydantoin (DCDMH) was employed since the originally used DCDPH results in the insoluble byproduct 1-chloro-5,5-diphenylhydantoin, adversely affecting the spectra of the evolving reaction mixture. (iv) to reduce the complexity of the initial kinetic studies, benzoic acid was omitted, although, as described in the SI, and later in the manuscript, including benzoic acid was illuminating with respect to the order of the substrate. These adjustments for the kinetic studies led to only a 5% drop in *ee* and presumably do not qualitatively change the reaction mechanism.

A detailed RPKA analysis of the chlorolactonization reaction revealed the following results (see SI for detailed experimental analysis and a brief theoretical description of RPKA in the context of asymmetric halogenation):

(a) The asymmetric chlorolactonization is *zero order* in alkene carboxylic acid **1**.

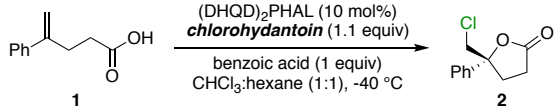

chlorohydantoin	Ar	*HalA* (Cl)[a] kcal/mol	%yield	%*ee*	k_{Ar} (s^{-1})
	4-Me-C_6H_4	274.3	86	88	1.6×10^{-6}
	C_6H_5	273.8	78	88	2.1×10^{-6}
	2-F-C_6H_4	272.4	67	88	2.4×10^{-6}
	4-CN-C_6H_4	266.3	78	84	5.6×10^{-6}
	4-NO_2-C_6H_4	265.2	71	86	7.4×10^{-6}

[a]Calculated at the B3LYP/6-31G*/SM8 ($CHCl_3$) level of theory.

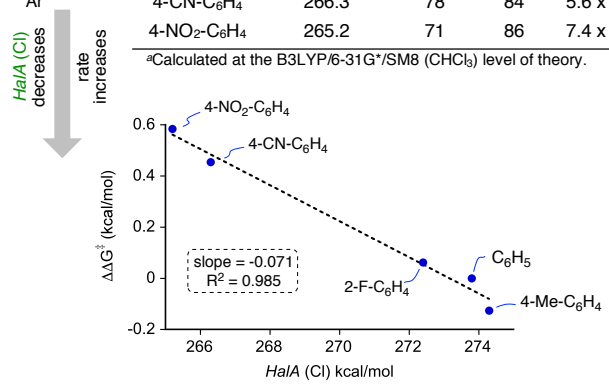

Figure 2. Electronic perturbation at the *N*1 substituent of chlorohydantoins affecting the rate of chlorolactonization. The plot represents the linear variation of $\Delta\Delta G^{\ddagger} = -RT\ln(k_{Ar}/k_{Ph})$, relating the experimentally determined rate constants (k_{Ar}) with the theoretically calculated absolute *HalA* (Cl) values.

(b) The reaction shows *first order* dependence with respect to the catalyst $(DHQD)_2PHAL$ and the chlorenium ion donor-DCDMH.

(c) The reaction does not suffer from any catalyst deactivation or product inhibition, as demonstrated by 'the same excess' experiments.

(d) Addition of an external carboxylic acid such as benzoic acid or an inert alkenoic acid, that can potentially compete with the substrate's binding to the catalyst's active site, retards the overall rate of the reaction.

The above observations can be summarized as follows:

$$Rate = k\,[(DHQD)_2PHAL]^1[DCDMH]^1[\mathbf{1}]^0$$

The fact that the reaction is zeroth order in substrate **1** (4-phenylpent-4-enoic acid) suggests that the catalyst is saturated, binding **1** rapidly to the basic quinuclidine moiety to form the strongly hydrogen-bonded acid-base adduct. As detailed further below, this **resting state** species is a 1:2 complex of $(DHQD)_2PHAL$ and **1.**

Quantum chemical modeling of the reaction components and their interactions finds that quinuclidine has a substantially stronger affinity for alkenoic acid **1** (-15.8 kcal/mol) than for DCDMH (-10.6 kcal/mol; see inset Table in Figure 3). It is thus not surprising that alkene **1** outcompetes DCDMH for binding to the catalyst. NMR evidence further supports this conclusion: 1,3-dichlorohydantoin with $(DHQD)_2PHAL$ shows splitting of the CH_2 hydrogens into a diastereotopic pair, implying a complex formed with the chiral catalyst. However, addition of **1** completely reverses this complexation, returning the hydantoin spectrum to that of uncomplexed reagent.[40]

Collision of suitable conformations of the **resting state** complex $(DHQD)_2PHAL$-**1** with DCDMH results in chlorenium transfer to the alkene in a rate determining step (RDS, see SI for the detailed kinetic model that leads to the rate law and proposed catalytic cycle). This process may follow either of two paths: (a) formation of a β-chloromethyl carbenium ion **intermediate A** (Path A, Figure 3), or (b) a concerted addition *via* **transition state B**, to directly access the products (Path B, Figure 3). This latter Ad_E3-type process is an example of nucleophile assisted alkene activation (*NAAA*).[63]

In the absence of $(DHQD)_2PHAL$ or quinuclidine catalysts, the DCDMH and alkene **1** are essentially unreactive at -40 °C. Therefore, apart from controlling the enantioselectivity by providing a chiral pocket, the catalyst must also activate the alkene or the DCDMH (or both). To promote the stepwise pathway leading to **intermediate A**, the catalyst must activate the DCDMH to form the proposed chlorocarbenium ion intermediate. The potential viability of forming the ionic species depicted in **intermediate A** is supported by NMR evidence that quinuclidine can deprotonate 3-chloro-5,5-dimethyl hydantoin (MCDMH) (shaded box in Figure 3). Rapid cyclization, guided by the catalyst, would then afford the product. On the other hand, the concerted pathway via **transition state B**

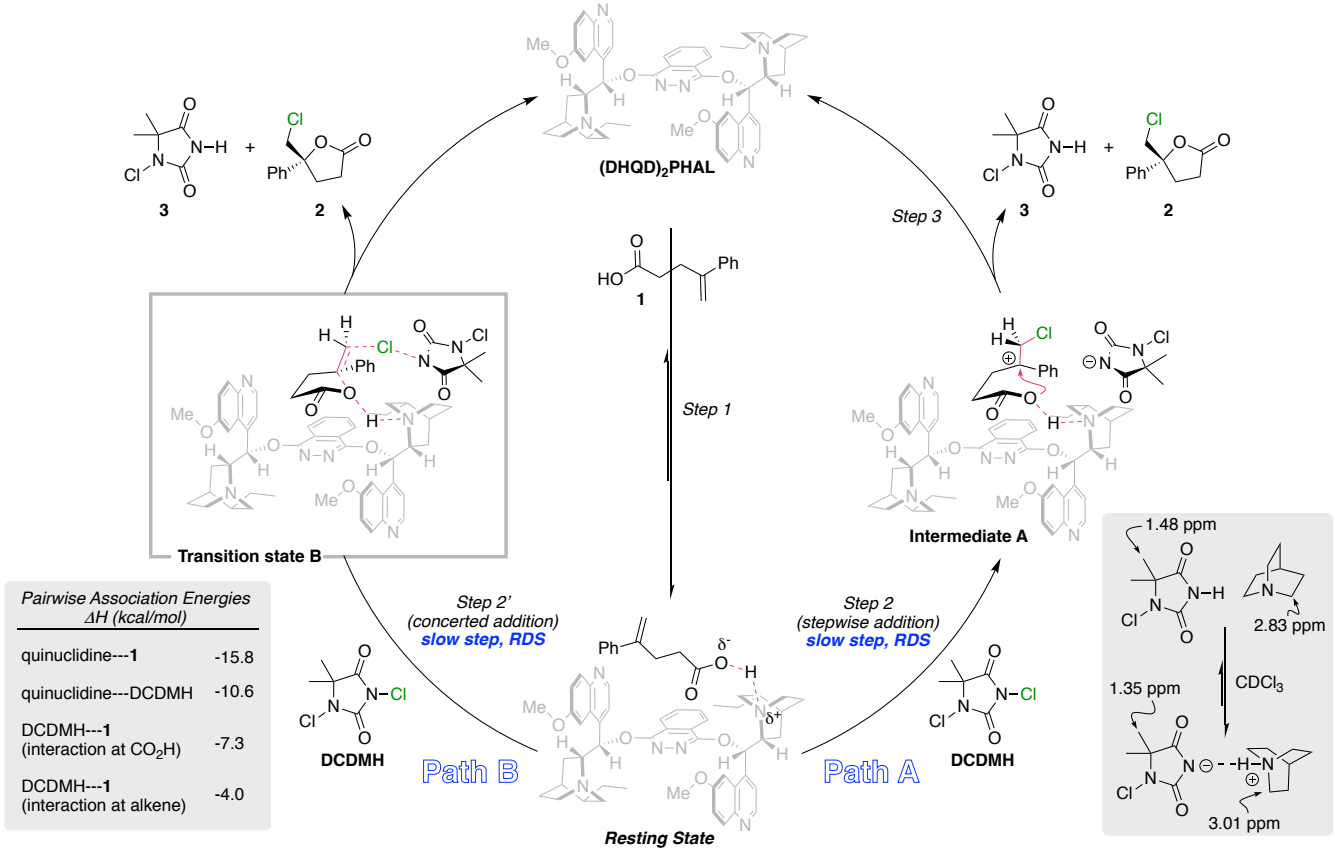

Figure 3. Putative catalytic cycle for $(DHQD)_2PHAL$ catalyzed chlorolactonization of alkenoic acid **1** (in the absence of benzoic acid additive). *Path A* depicts a stepwise addition via a carbocationic **intermediate A**. The shaded box on the right confirms the possibility of generating the ion-pair depicted in **intermediate A** (^1H NMR studies show that quinuclidine deprotonates 3-chloro-5,5-dimethyl hydantoin in $CDCl_3$). *Path B* depicts a possible one step concerted addition to the alkene **1**. NMR studies and computational modeling of the proposed intermediates and transition states are detailed in the following section. The left table insert displays calculated binding enthalpies of alkene **1**, DCDMH and quinuclidine (a truncated model for the catalyst). These pairwise association energies argue for the validity of the **resting state**. For clarity, only one alkenoic acid is shown bound to the catalyst, although experimental results indicate two molecules are bound at one time (*vida infra*).

hinges on the activation of the alkene, irrespective of additional activation of the chlorenium source.

In the case of stepwise cyclization, the cation closure (step three in Figure 3) could not be rate limiting as this would predict a buildup of cation intermediate, which is not observed. Also, reversible formation of the carbocation should scramble the stereochemistry of the alkene =CHD site in deuterium labeled substrate **1-D** (see Scheme 1), a process ruled out by the finding that recovered starting materials retain their stereochemical integrity.[4a] In the alternative event of a concerted addition *via NAAA* (**transition state B**), the concerted chlorenium ion attack and ring closure would directly form the chlorolactone product. In either case (Path A or B), the chlorenium ion delivery to the olefin (step 2 or 2') must be part of the rate-determining step.

The kinetic studies also helped clarify the role of the benzoic acid additive, which marginally increases the enantioselectivity. We surmise that its presence aids in maintaining the rigidity of the C_2-symmetric $(DHQD)_2PHAL$ catalyst (see next section for validation of this hypothesis by NMR and X-ray studies), and perhaps also aids in shuttling the protons required to neutralize the byproduct hydantoin anions, especially toward the end of the reaction when the concentration of **1** is low. Consistent with this idea, benzoic acid addition at an equimolar ratio to substrate lowers the rate of chlorolactonization (see SI for experimental details); presumably benzoic acid competes with 4-phenylpent-4-enoic acid **1** for binding in the catalyst's active site (*vida infra*). This interpretation gained support from RPKA studies with benzoic acid added, which raised the measured order of the alkene from zero to 0.5 in the rate equation. This change is expected due to the fact that alkene **1** has to compete with the benzoic acid for binding in the catalyst, making its concentration relevant with respect to the rate. The following is the observed rate law in presence of benzoic acid:

$$Rate = k\,[(DHQD)_2PHAL]^1[DCDMH]^1[\mathbf{1}]^{0.5}$$

To further explore the proposed catalytic cycle, we resorted to competition studies (Figure 4). Prior analysis of the catalytic asymmetric chlorolactonization methodology revealed that 4-(4-(trifluoromethyl)phenyl)pent-4-enoic acid **3** is one tenth as reactive as **1**.[40] Nonetheless, the trifluoromethyl substituent should not interfere with binding, as other sterically comparable substrates behaved well under the same reaction conditions. If substrate **3** binds to the catalyst to form an unreactive analogue of the **resting state**, it should serve as a competitive inhibitor, decreasing the concentration of the reactive complex with substrate **1**. Indeed, as shown in Figure 4, the chlorolactonization of **1** was slowed dramatically (decreased by 58%) upon addition of one equivalent of **3** to a 1:1 mixture of **1** and DCDMH with 1.5 mol% catalyst.

A similar competition study was performed between 4-phenylpent-4-enoic acid **1** and 4-(3-nitrophenyl)pent-4-enoic acid **4**, known to be a slow substrate. With a 1:1:1 mixture of substrates **1**, **4** and DCDMH under 1.5 mol% catalyst loading, the rate of the chlorolactonization of **1** was decreased by 71% (Figure 4). At a 1:1 ratio of inhibitor **4** to substrate **1**, a 50% decrease in rate would suggest similar binding affinity of **4** and **1** with $(DHQD)_2PHAL$; the larger observed inhibition suggests a stronger complexation with **4**, consistent with the formation of a putatively stronger π-acid-base complex.

Further evidence supporting the idea that chlorine delivery from the hydantoin to **1** is rate-determining may be found in the effects of structural variations in the hydantoin chlorenium donors. As noted

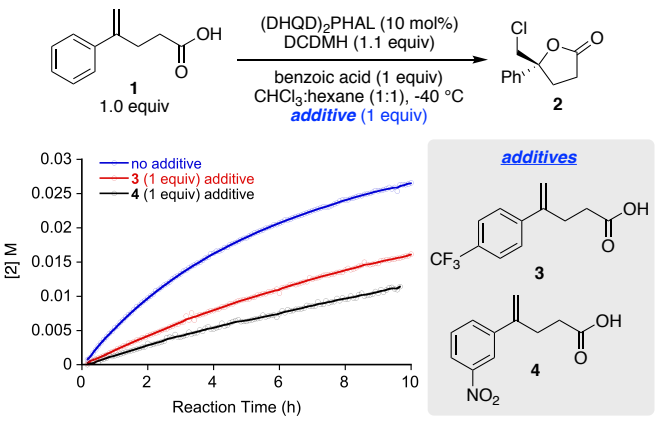

Figure 4. Rate of formation of product **2** in presence of alkenoic acids **3** and **4**. The reduced rates imply **3** and **4** are competitive inhibitors of the catalyst, presumably binding to the active site and retarding the binding of substrate **1**.

earlier (Figure 2), the *N*3 chlorine is activated when the *N*1 substituent of DCDMH is an electron withdrawing group (EWG). As quantified by the *HalA* values, stronger EWGs on *N*1 accelerate the reaction, consistent with chlorine delivery to **1** in the RDS. A related result is that chiral chlorohydantoins show match/mismatch effects in reaction, pointing to direct involvement of the chlorenium delivery reagent in the chlorocyclizations.[57]

To probe the involvement of the carboxylic acid moiety in the rate determining step, chlorocyclization of the deuterated 4-phenylpent-4-enoic acid **1-OD** (RCO_2D) was studied and compared to the same reaction with unlabeled substrate **1**. An inverse isotope effect ($k_H/k_D = 0.82$, see SI) was measured, suggesting that the carboxylate plays a direct role in the reaction. Considering *Path A*, the change from H to D should not lead to the observed KIE, as the electrophilic transfer of the chlorenium ion is ostensibly insensitive to the nature of the hydrogen-bonded nucleophile. On the other hand, the concerted *Path B* via **transition state B** would presumably be accelerated by the H to D change, as the carboxylate oxygen's, and therefore the alkene's nucleophilicity is more activated as a consequence of the increased acidity of **1-OD** vs **1-OH**.

Overall, reaction progress kinetic analysis (RPKA), competition, reagent, and isotope studies find that (a) rate is first order in catalyst and in DCDMH, but zero order in substrate; (b) chlorenium donor ability and asymmetry characteristics affect reaction rates; and (c) the carboxylic acid's hydrogen isotope also modulates reaction rate. The implication is that the rate-determining step involves chlorenium transfer and the carboxylic acid's degree of deprotonation.

2. Resting state of the catalytic cycle

With the elementary steps of the catalytic cycle deduced from the kinetic findings, we undertook NMR and computational studies to gain structural insight into intermediates and transition states along the reaction paths. Our first target in this process was the **resting state** (catalyst-substrate complex) of the catalytic cycle.

A comprehensive conformational search of the free catalyst using molecular mechanics and density functional simulations revealed three low energy conformational orientations for the two sidechains on the phthalazine (see SI for computational details). These showed H_aCCH_b dihedral angles of roughly 80° and 170°, consistent with prior NMR and theoretical work.[64-66] Figure 5 (left) shows a DFT-B3LYP/6-31G* (gas) minimized structure of

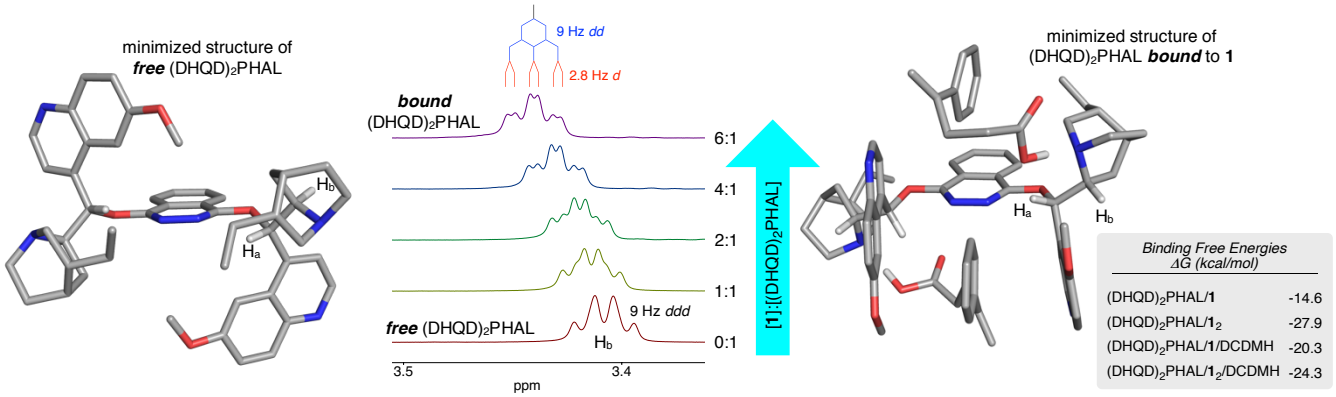

Figure 5. Conformational changes observed upon binding of **1** to $(DHQD)_2PHAL$. The left model represents the minimized structure of free $(DHQD)_2PHAL$ with H_aCCH_b dihedral angle ~170°, supported by the 9 Hz coupling of H_b with H_a. H NMR titration induces a change in the H_b/H_a coupling from 9 to <3 Hz with the addition of the alkenoic acid **1**. The model on the right depicts a minimized structure of the catalyst bound to two alkenoic acid **1**, where the two H_aCCH_b dihedral angle are 73.8° and 80.7°. The dihedral angles of the bound catalyst fit well with the observed smaller coupling constant for H_a/H_b. Computed binding free energies for complexation of the first and second alkenoic acids **1**, and for DCDMH with $(DHQD)_2PHAL$ are shown in the shaded box.

$(DHQD)_2PHAL$ with a H_aCCH_b dihedral of 169.4°. This is consistent with the NMR of free $(DHQD)_2PHAL$, where the H_b resonance exhibits a *ddd* with three equivalent 9 Hz coupling constants. Dihedral angles between H_b and the methylene protons in the quinuclidine ring lead to the anticipated 9 Hz coupling. Thus, the third 9 Hz coupling of H_b is ascribed to its interaction with H_a, resulting from the *anti* orientation of the two protons.

Table 1. ^1H NMR analysis of alkenoic acid **5** and its complexes with $(DHQD)_2PHAL$ and quinuclidine at -40 °C in $CDCl_3$.

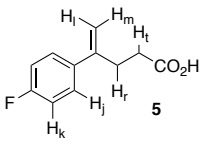

quinuclidine (quin.) 

proton	δ (ppm)	Δδ with $(DHQD)_2PHAL$	Δδ with quin.
H_t	2.52	-0.52	-0.19
H_r	2.80	-0.43	-0.06
H_m	5.06	-0.46	-0.04
H_l	5.25	-0.54	-0.04
H_j	7.36	-0.23	+0.04
H_k	7.01	-0.29	-0.06

Titration of $(DHQD)_2PHAL$ with substrate **1** lowers the catalyst's H_a-H_b coupling constant from 9 to <3 Hz, suggesting a conformation with an averaged H_aCCH_b dihedral angle close to 90°. This geometry, as depicted in Figure 5, also orients the quinuclidine N toward the chiral cleft of the catalyst. Furthermore, the 1:1 catalyst complex exhibits broad peaks which sharpen on addition of another equivalent of alkenoic acid suggesting that in the **resting state**, the catalyst binds two alkenes. Finally, conformational searching using the MMFF94 force field, followed up by B3LYP-D3/6-31G*/postSMD($CHCl_3$) structural optimization of the $(DHQD)_2PHAL$ bound with two alkenoic acids found calculated binding free energies for the first and second molecules of **1** in $(DHQD)_2PHAL$ of -14.6 and -13.3 kcal/mol, respectively. Among the lowest energy complex minima, the structure shown at right in Figure 5 is used here as the **resting state** catalyst model; this structure has H_aCCH_b dihedral angles of 73.8° and 80.7°, consistent with the <3 Hz coupling of H_a with H_b in the NMR of the fully saturated complex.

Given the desymmetrization observed in the NMR of dichlorohydantoin interacting with the catalyst, one might expect that DCDMH binding would compete for the catalyst active site. However, for both the empty and singly occupied forms of the catalyst, the -14.6 and -13.3 kcal/mol binding energies of an additional acid substantially outcompete the -5.7 kcal/mol binding free energy of a molecule of DCDMH. Interacting with the doubly occupied **resting state**, the association of DCDMH is even weaker, as shown by the free energy values in Figure 5.

Further structural data on the **resting state** complex were obtained from NMR studies of a 2:1 mixture of 4-(4-fluorophenyl)pent-4-enoic acid **5** and $(DHQD)_2PHAL$ in $CDCl_3$ carried out at -40 °C. Carboxylic acid **5** was used as a substitute for **1** since its aromatic protons (ortho to fluorine) do not overlap with the aromatic protons of the catalyst. Table 1 compares the ^1H NMR chemical shifts of the substrate with and without $(DHQD)_2PHAL$ present. It is notable that the vinylic protons and also two methylene groups of the alkenoic acid **5** are shielded by ~0.5 ppm upon complexation with catalyst. We interpret this shielding as a combination of two effects: (a) deprotonation of the carboxylic acid and (b) binding in the cleft of the catalyst. To distinguish these contributions, ^1H NMR spectra of **5** were taken with quinuclidine in $CDCl_3$. There, it was the methylene group adjacent to the carboxylate moiety that showed the highest upfield shift (0.19 ppm). The other protons' shifts showed at most slight changes (~0.04 ppm). Thus, acid-base complex formation does not account fully for the large shielding seen with the catalyst–bound substrate.

To further probe the interactions between the substrate and the catalyst, ROESY experiments using the methods described by Bodenhausen *et al.*[67-69] found correlations between protons of **5** and $(DHQD)_2PHAL$ offering further insights into binding. As depicted in Figure 6, ROESY correlations, leading to average distances are grouped into intramolecular and intermolecular correlations. The

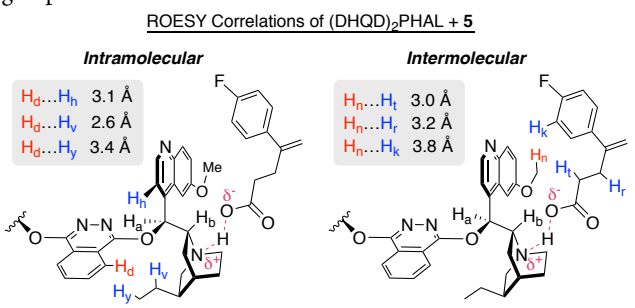

Figure 6. Intramolecular and intermolecular ROESY correlations of **5** bound to $(DHQD)_2PHAL$. The intramolecular correlations place the ethyl group near the phthalazine ring, while the methoxy shows close intermolecular relations with the substrate methylene units. These interactions are present in the lowest energy conformation of $(DHQD)_2PHAL$ (see Figure 5, bound structure).

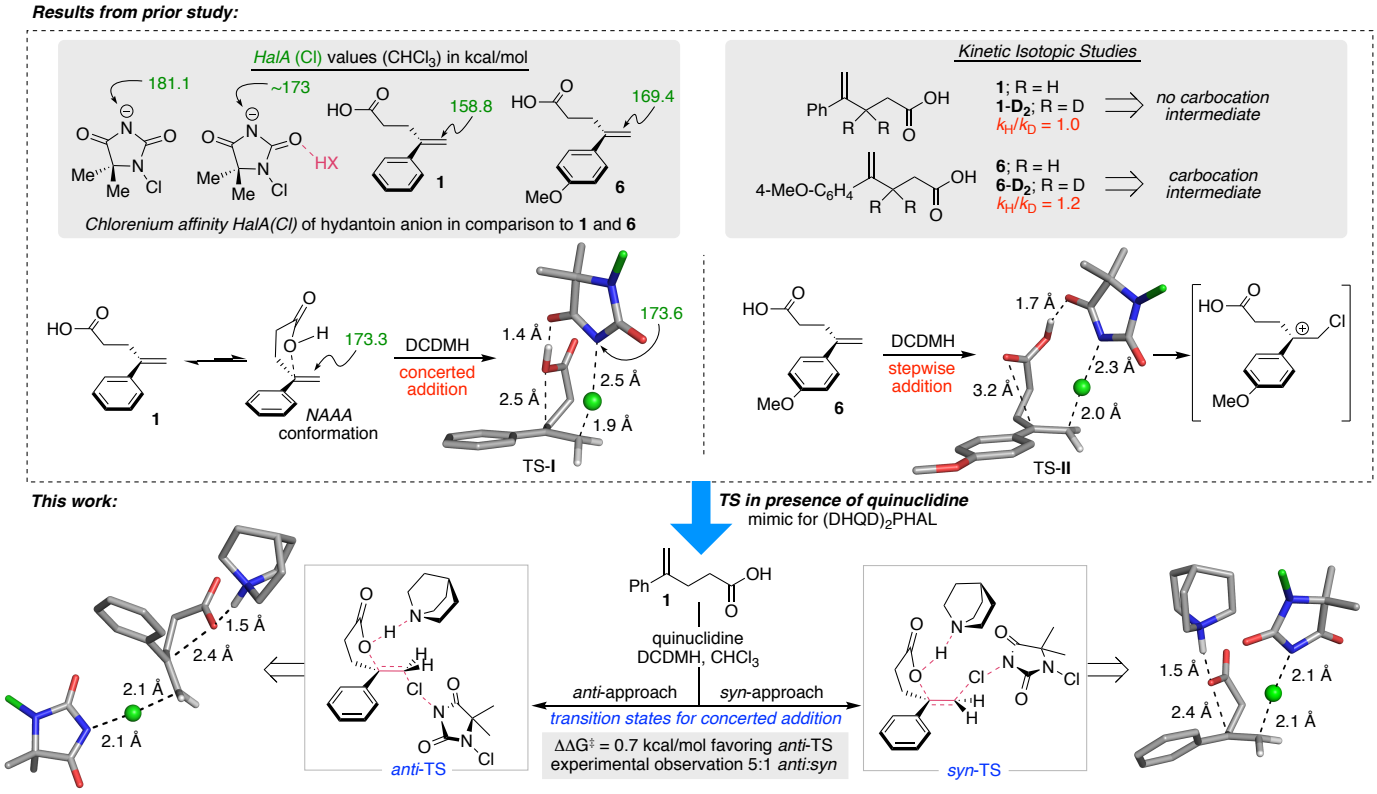

Figure 7. a. Prior work illustrating experimental evidences that support concerted addition to an alkene b. Transition states leading to *syn* and *anti*-addition for quinuclidine catalyzed chloro-lactonization. Calculated using density functionals B3LYP-D3/6-31G* SM8 ($CHCl_3$)

distances derived for the intramolecular interactions fit well with the minimized structure of the catalyst, illustrated in Figure 5. Probing intermolecular interactions, the OMe sidechains of the quinoline group (H_n) showed contacts with the substrate's methylene (H_r and H_t) and phenyl protons (H_k). This also matches well with the calculated **resting state** model, depicted in Figure 5, where the calculated distances fall well within the ROESY measured values (H_n/H_t 2.6 Å calc'd, 3.0 Å expt, H_n/H_r 2.5 calc'd, 3.2 Å expt, H_n/H_k 2.9 Å calc'd, 3.8 Å expt). The ROESY verified model for the **resting state** shown in Figure 5 illustrates carboxylate binding to the protonated quinuclidine moiety, positioning the vinylic protons in the shielding regions of the quinoline rings, which leads to their observed upfield shifts.

As a C_2 symmetric cinchona alkaloid, $(DHQD)_2PHAL$ can potentially bind to two substrates at the same time (as depicted in Figure 5). Consistent with this idea, when $(DHQD)_2PHAL$ is treated with only one equivalent of the alkenoic acid **1**, the ^1H NMR peak broadening at room temperature clearly suggests loss of structural symmetry due to partial occupancy of the substrate. The spectra sharpen up in the presence of two equivalents of **1**. These results support a picture in which $(DHQD)_2PHAL$ requires two substrates (or other carboxylic acids) to maintain its conformational rigidity in the C_2-symmetric *anti*-open form. On the other hand, addition of four equivalents of alkenoic acid to $(DHQD)_2PHAL$ resulted in an averaged spectrum for the substrates, indicating fast equilibrium (on the NMR time scale) between bound and free forms of the alkenoic acid, while the catalyst's spectra remained sharp. Similar behavior is seen with benzoic acid (see SI for NMRs of $(DHQD)_2PHAL$ with benzoic acid).

To further explore the stoichiometry of complexation, $(DHQD)_2PHAL$ was treated with two equivalents of a 1:1 mixture of alkenoic acids **1** and **4**. This NMR experiment showed shielding behavior for both **1** and **4** similar to that seen in 2:1 substrate:catalyst mixtures with the individual substrates. If catalyst had only a single binding site, such mixtures should show more shielding of resonances of the more tightly bound alkenoic acid. Since the same degree of chemical shift is observed in the above case with the spectra being well-resolved, it appears that the catalyst binds both substrates in a 1:1:1 complex without competition. This 2:1 binding model is in accord with the reactivity results involving **1**, **3**, and **4** previously shown in Figure 4, and with the calculated binding energetics in Figure 5. As discussed further below, the 2:1 complex may undergo attack by the chlorenium ion donor on either of the two essentially independently bound substrate molecules; it is thus the substrate for attack by the chlorenium ion donor.

An alternative scenario might involve dissociation to an active 1:1 complex, with the catalytically incompetent 2:1 complex serving simply as an off-cycle reservoir. In this scenario, however, the initial rate would not be the same for two reactions with different starting concentrations, such as the different excess experiments carried out in this study. We would anticipate the reaction with a higher concentration of the starting alkene to have a smaller initial rate. This behavior is not observed (see Figure S1 and the description of kinetic models in the SI).

Although we were unable to obtain crystals of the **resting state** itself, we were able to co-crystallize the catalyst $(DHQD)_2PHAL$ with benzoic acid. This crystal structure displayed essentially the conformation deduced from the NMR studies (see SI for crystal structure), with the two H_aCCH_b dihedral angle being 73.7° and 77.6°.

3. Structural insights into transition state B

To understand the asymmetric induction achieved in the $(DHQD)_2PHAL$-catalyzed chlorocyclization of **1** with DCDMH, a model of the interaction of the chlorenium ion donor with the **resting state** is needed, which must entail both activation and asymmetric specificity. The combination of substrate **1** with DCDMH alone is essentially unreactive (at -30 °C); a basic catalyst, such as quinuclidine or $(DHQD)_2PHAL$ is needed to promote the reaction. Also, as noted earlier, both rate and stereoselectivity are affected by electronic and stereochemical variations in the dichlorohydantoins used. Thus, the ring-forming reaction involves both the state of carboxylate deprotonation, and the identity of the chlorine donor.

One path that might be envisioned is indirect chlorine transfer to substrate via a chlorinated $(DHQD)_2PHAL$. This can be ruled out as it predicts that the enantioselectivity should be independent of the chlorenium ion source (hydantoin) as the *N*-chloroquinuclidinium form of $(DHQD)_2PHAL$ would now serve as the active *in situ* generated halogenating reagent. Also, as assessed in terms of *HalA* (Cl) values, chlorenium ion transfer to the quinuclidine nitrogen in the catalyst would be strongly endothermic (Δ*HalA* (Cl) 24.0 kcal/mol in $CHCl_3$), even when the stabilizing effects of tight ion pairing and solvation are included in the calculation.

Evidence for concerted addition (*NAAA*) pathway

Without assistance, chlorenium transfer from DCDMH to the alkene would be unfavorable (Δ*HalA* (Cl) = 22.3 kcal/mol in $CHCl_3$) (see *HalA* values in Figure 7). Despite its low *HalA*, alkene **1** does slowly react with DCDMH. However, the rate is accelerated greatly in the presence of a basic catalyst such as quinuclidine. This strongly suggests that the catalyzed halocyclization of **1** proceeds via a nucleophilic activated alkene addition (*NAAA*) mechanism. Previous reports on chlorolactonization (summarized in Figure 7, dashed box) have noted that a low energy barrier pathway via concerted addition can be triggered when the substrate adopts conformations with the anionic carboxylate oxygen atom near the alkene moiety. This close proximity of the nucleophile sharply enhances the alkene halenium affinity, enabling capture of the chlorenium ion from its donor, as the nucleophile approach now stabilizes for the developing charge in the alkene sp^2 carbon. This view is verified further by the contrasting isotope effects seen in the uncatalyzed reactions of DCDMH with alkenes **1** and **6** (Figure 7, dashed box). Here, in **1**, replacement of the protons vicinal to the putative carbenium site with deuterium showed no observable kinetic isotopic effect (k_H/k_D = 1.0).[63] As depicted in Figure 7, TS-**I** illustrates the concerted transition state with bond distances that indicate a one-step, asynchronous addition of the chlorenium and the carboxylate to the olefin. In the case of **6**, the 4-methoxy analog of **1**, the alkene's nucleophilicity is inherently enhanced enough that the nucleophile-assisted pathway is unimportant; uncatalyzed reaction of **6** with DCDMH is much faster as compared to **1**. However, as expected for a stepwise pathway via a carbocationic intermediate, reaction of alkene **6** displayed a significant secondary kinetic isotopic effect (k_H/k_D = 1.2). In contrast to the concerted addition calculated for alkene **1**, TS-**II** depicts the attack to form the carbocation in the stepwise addition of the chlorenium ion to substrate **6**. The *HalA* (Cl) values of **1** and **6** (158.8 and 169.4 kcal/mol) differ by >10 kcal/mol, supporting the formation of a carbocation intermediate. The *HalA* (Cl) value of **6** closely matches that of the hydrogen-bonded MCDMH anion (~173 kcal/mol), consistent with unassisted chlorenium capture by **6** to form the carbocation, an action too endothermic for olefin **1** without further activation.

The *m*-NO_2 analogue of **1**, alkene **3**, is intrinsically deactivated and unreactive towards DCDMH, hinting that *NAAA* can only offer so much activation if there are strong inherent factors retarding the intrinsic nucleophilicity of the alkene. Though it appears quite general for otherwise nonpolarized alkenes, the concerted *NAAA* mechanism evidently strikes a fine balance. With the experimental evidence firmly indicating concerted addition to the alkene **1**, transition states with quinuclidine as well as $(DHQD)_2PHAL$ as a catalyst were computationally modeled and analyzed in the following section.

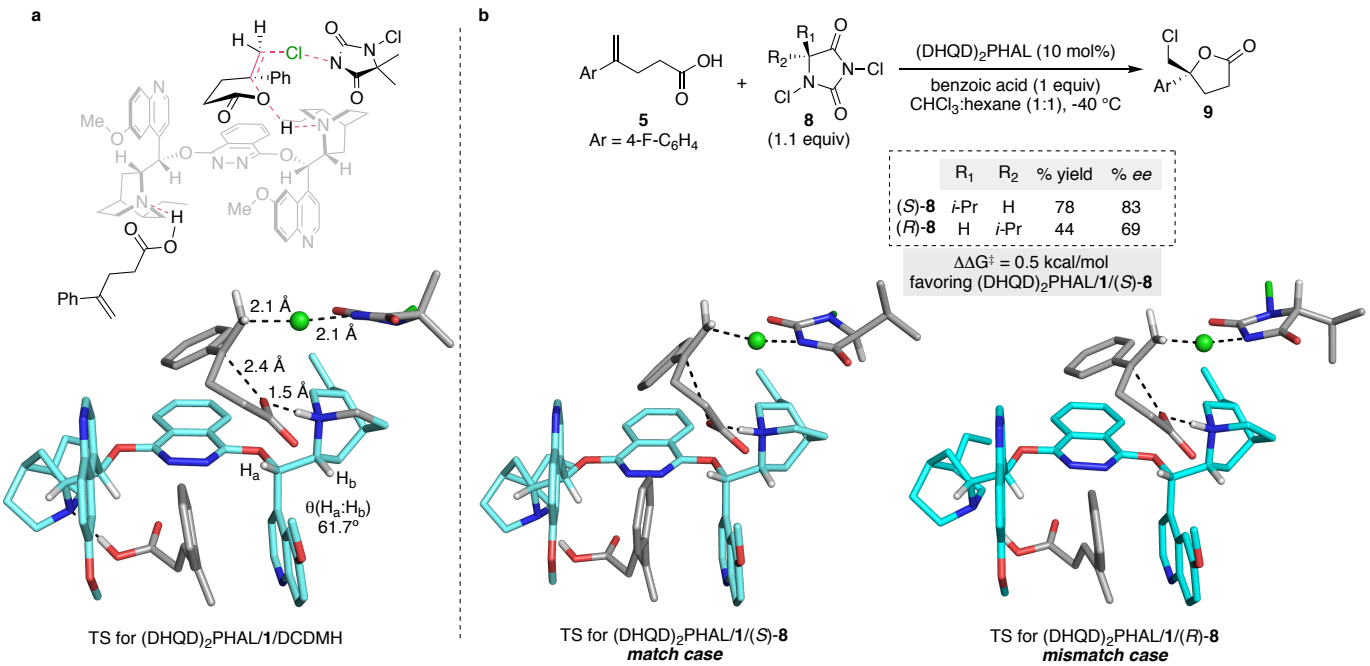

Figure 8. Transition states for $(DHQD)_2PHAL$ catalyzed chloro-lactonization using DCDMH and the chiral chlorenium reagent. The non-degeneracy of the two transition states conforms with the previously reported matched-mismatched selectivity. Structures were calculated using the dispersion-corrected density functional method B3LYP-D3, with all optimizations carried out in SMD simulated $CHCl_3$. This scheme is denoted B3LYP-D3/6-31G*/SMD($CHCl_3$).

Quinuclidine-catalyzed TS for *syn* and *anti* chlorocyclization

For the quinuclidine catalyzed reaction, transition structures for the lowest energy *syn* and *anti* concerted addition pathways were identified and optimized. (Figure 7, bottom). In search of optimized structures, conformational analyses using the MMFF94 force field provided poses, which were further refined via B3LYP-D3/6-31G*/postSMD ($CHCl_3$) calculations. Though the developing negative charge on the hydantoin ring in the *syn* TS benefits from proximity to the partially positive protonated quinuclidine, that advantage is outweighed by the steric freedom of approach from the far side (*anti* approach). In the $CHCl_3$ "solvent" as represented by the SMD dielectric continuum simulation, the *anti*-addition pathway is found to be 0.7 kcal/mol lower in energy than its *syn* partner, a result consistent with experimental findings. Both structures show similar parameters, with the developing C-Cl and C-O bond lengths slightly longer in the *anti* (2.2, 2.6 Å) than in the *syn* case (2.1, 2.4 Å). All attempts to initiate chlorenium atom transfer from DCDMH to **1** were monotonically endothermic in conformations that did not place the nucleophilic carboxylate moiety nearby (Figure 7, bottom). This implies that a stable β-chloromethyl carbenium ion intermediate is not a minimum along the reaction coordinate as would be expected for the stepwise mechanism.

The experimentally observed *syn*:*anti* ratio for quinuclidine catalyzed chlorocyclization of **1**-**D** is 1:5.[56] This agrees with the discussion above, and also with the calculated difference in activation energies computed for the *syn* and *anti* TS structures shown in Figure 7 ($\Delta\Delta G^{\ddagger}$ = 0.7 kcal/mol).

Modeling of the *syn*-addition TS for $(DHQD)_2PHAL$ catalyzed reactions

Having identified the lowest energy TS structures for quinuclidine-catalyzed chlorocyclization of **1**, we proceeded to model the *syn* structure into the optimized geometry of $(DHQD)_2PHAL$, re-optimizing at the B3LYP-D3/6-31G* level of theory. The reader is reminded that the asymmetric catalyzed chlorolactonization of **1**-**D** favors the *syn* adduct **2**-**D** (*syn*:*anti* ratio ~9:1).[56] The energy of activation (10.5 kcal/mol) and partial bond lengths (2.4 Å for C-O and 2.1 Å for C-Cl) for the lowest energy $(DHQD)_2PHAL$ catalyzed transition state were comparable to the quinuclidine catalyzed addition (Figure 8a). The acute H_aCCH_b dihedral angle of 61.7° in the TS effectively oriented the quinuclidine towards the center of the catalyst allowing for the alkenoic acid to sit inside the chiral pocket as it further enjoys π-π-stacking with the phthalazine linker. This dihedral angle also fits well with the NMR studies depicted in Figure 5 for $(DHQD)_2PHAL$ bound to **1**. As illustrated in Figure 8a, the *Re* face of the alkene is now readily accessible by both the chlorenium ion donor and the quinuclidine-activated carboxylate nucleophile, the simultaneous addition of which leads to the experimentally observed major *syn* enantiomer. Computational searches for *NAAA*-type TS structures leading to the minor products were much less successful; those products may well arise via more complex stepwise paths, and further studies in this direction are deferred to a future detailed computational analysis.

Prior studies have demonstrated that chlorolactonization using chiral chlorohydantoins exhibits matched-mismatched behavior when used with $(DHQD)_2PHAL$ (Figure 8b, table in dashed box). This provides further support for the hydantoin's direct involvement in the rate determining step as the chlorenium source. To connect our computational results to these experimental findings, we reoptimized the $(DHQD)_2PHAL$ catalyzed transition state with the two enantiomers of the chiral hydantoin **8** and alkene **1**. Consistent with the experimental findings, the TS calculated with the (*R*)-**8** (mismatch) shows steric crowding of the isopropyl group with the quinuclidine moiety of $(DHQD)_2PHAL$, presumably magnified as the hydantoin is approaching the **resting state** prior to reaching the TS. The (*S*)-congener (match), however, has a more relaxed approach, having the isopropyl group pointed in the opposite direction. This is also represented in the activation energies for each transition state, with the match TS having a slightly lower barrier ($\Delta\Delta G^{\ddagger}$ = 0.5 kcal/mol). Owing to less steric conflict with the catalyst, the approach of (*S*)-**8** to the olefin is also more linear, avoiding the DCDMH distortion seen in the TS from the (*R*) isomer.

Summary

Reaction progress kinetic analysis (RPKA) and competition studies revealed the delivery of chlorenium ion to the olefin as a key feature of the rate determining step (RDS). These kinetic studies also define the order of each reagent and consequently the rate equation of this catalytic reaction both in the presence and absence of the benzoic acid: rate = $k[(DHQD)_2PHAL][DCDMH]$. Moreover, these studies were conducted at concentrations relevant to the optimized standard protocol, obviating the need for extrapolations outside the range studied. The observed inverse isotope effect (acid catalysis) suggests that the alkene-COOD is more activated for DCDMH attack in **transition state B** than alkene-COOH. Between the kinetic results, ROESY NMR studies, X-ray structures, and DFT analysis, we propose a **resting state** model in which two molecules of substrate **1** occupy the binding pockets of $(DHQD)_2PHAL$. In the proposed catalytic cycle (Figure 3), the alkene face that is ultimately chlorinated is exposed to solution, allowing collision with DCDMH. Ring closure is achieved when the backbone chain achieves a conformation placing C-4 near the partially negatively charged carboxylate oxygen, activating the olefin for the concerted *NAAA* closure. The *syn* preference reflects the electrostatic attraction between the developing negative charge on the hydantoin and the positively charged quinuclidinium ion. These mechanistic investigations, coupled with our previously reported labeling studies, suggest that the rate-determining and enantioselectivity-determining events occur together in the predominant pathway. Taken together, the experimental results were combined with an initial DFT analysis that provided structural insight into the **resting state** model and the corresponding **transition state B**. Overall, using the asymmetric chlorolactonization of **1** as a proof of principle, a toolbox of analytical techniques has been successfully optimized and applied to probe the nuances underlying the $(DHQD)_2PHAL$ catalyzed halofunctionalization of olefins. These mechanistic studies have established an optimal range of alkene *HalA* values over which concerted reactions dominate, firmly defining both relative and absolute stereochemical relationships. This conceptual framework and set of tools for reaction assessment will serve as a guide, in a broad sense, to the emerging field of catalytic stereoselective halofunctionalizations of olefins. More specifically, the localized interactions identified in exploring these chlorolactonization reaction paths point the way to key features needed in the design of simplified organocatalysts.

ASSOCIATED CONTENT

Supporting Information. Experimental details, *HalA* calculations, characterization data, DFT computational data and MS

office excel template for RPKA analysis. This material is available free of charge *via* the Internet at http://pubs.acs.org.

AUTHOR INFORMATION

*Corresponding Authors

babak@chemistry.msu.edu
jackson@chemistry.msu.edu

Author Contributions

†These authors contributed equally.

ORCID

Babak Borhan: 0000-0002-3193-0732

Notes

The authors declare no competing financial interest.

ACKNOWLEDGMENT

Generous support was provided in part by the NIH (GM110525) and the NSF (CHE-1362812). The authors thank Dr. Richard Staples for the X-ray structure of $(DHQD)_2PHAL$ complexed with benzoic acid. The authors acknowledge the work of undergraduates Melissa Mu, Christopher Rahn, Eduord Toma, and Lindsey Kiilsika for their contributions to this work.

Present Address

‡Department of Chemistry, Clemson University, Clemson, South Carolina, 29634, United States.

REFERENCES

(1) Cresswell, A. J.; Eey, S. T.; Denmark, S. E. Catalytic, Stereoselective Dihalogenation of Alkenes: Challenges and Opportunities. *Angew. Chem. Int. Ed. Engl.* **2015**, *54*, 15642.

(2) Abe, H.; Fukazawa, N.; Kobayashi, T.; Ito, H. Indium chloride mediated chlorolactonization: construction of chlorinated lactone fragments. *Tetrahedron* **2013**, *69*, 2519.

(3) Ahmad, S. M.; Braddock, D. C.; Cansell, G.; Hermitage, S. A.; Redmond, J. M.; White, A. J. P. Amidines as potent nucleophilic organocatalysts for the transfer of electrophilic bromine from N-bromosuccinimide to alkenes. *Tetrahedron Lett.* **2007**, *48*, 5948.

(4) Brucher, O.; Bergstrasser, U.; Kelm, H.; Hartung, J.; Greb, M.; Svoboda, I.; Fuess, H. Controlling 6-endo-selectivity in oxidation/bromocyclization cascades for synthesis of aplysiapyranoids and other 2,2,6,6-substituted tetrahydropyrans. *Tetrahedron* **2012**, *68*, 6968.

(5) Cardillo, G.; Orena, M. Stereocontrolled cyclofunctionalizations of double-bonds through heterocyclic intermediates. *Tetrahedron* **1990**, *46*, 3321.

(6) Castellanos, A.; Fletcher, S. P. Current Methods for Asymmetric Halogenation of Olefins. *Chem. Eur. J.* **2011**, *17*, 5766.

(7) Chen, F.; Tan, C. K.; Yeung, Y. Y. C-2-Symmetric Cyclic Selenium-Catalyzed Enantioselective Bromoaminocyclization. *J. Am. Chem. Soc.* **2013**, *135*, 1232.

(8) Chen, G.; Ma, S. Enantioselective Halocyclization Reactions for the Synthesis of Chiral Cyclic Compounds. *Angew. Chem. Int. Ed.* **2010**, *49*, 8306.

(9) Denmark, S. E.; Burk, M. T. Lewis base catalysis of bromo- and iodolactonization, and cycloetherification. *Proc. Natl. Acad. Sci. U. S. A.* **2010**, *107*, 20655.

(10) Denmark, S. E.; Burk, M. T. Enantioselective Bromocycloetherification by Lewis Base/Chiral Bronsted Acid Cooperative Catalysis. *Org. Lett.* **2012**, *14*, 256.

(11) Dowle, M. D.; Davies, D. I. Synthesis and synthetic utility of halolactones. *Chem. Soc. Rev.* **1979**, *8*, 171.

(12) Fang, C.; Paull, D. H.; Hethcox, J. C.; Shugrue, C. R.; Martin, S. F. Enantioselective Iodolactonization of Disubstituted Olefinic Acids Using a Bifunctional Catalyst. *Org. Lett.* **2012**, *14*, 6290.

(13) Garnier, J. M.; Robin, S.; Rousseau, G. An approach to enantioselective 5-endo halo-lactonization reactions. *Eur. J. Org. Chem.* **2007**, 3281.

(14) Grossman, R. B.; Trupp, R. J. The first reagent-controlled asymmetric halolactonizations. Dihydroquinidine-halogen complexes as chiral sources of positive halogen ion. *Can. J. Chem.* **1998**, *76*, 1233.

(15) Haas, J.; Bissmire, S.; Wirth, T. Iodine monochloride-amine complexes: An experimental and computational approach to new chiral electrophiles. *Chem. Eur. J.* **2005**, *11*, 5777.

(16) Haas, J.; Piguel, S.; Wirth, T. Reagent-controlled stereoselective iodolactonizations. *Org. Lett.* **2002**, *4*, 297.

(17) Ikeuchi, K.; Ido, S.; Yoshimura, S.; Asakawa, T.; Inai, M.; Hamashima, Y.; Kan, T. Catalytic Desymmetrization of Cyclohexadienes by Asymmetric Bromolactonization. *Org. Lett.* **2012**, *14*, 6016.

(18) Jaganathan, A.; Garzan, A.; Whitehead, D. C.; Staples, R. J.; Borhan, B. A Catalytic Asymmetric Chlorocyclization of Unsaturated Amides. *Angew. Chem. Int. Ed.* **2011**, *50*, 2593.

(19) Jaganathan, A.; Staples, R. J.; Borhan, B. Kinetic Resolution of Unsaturated Amides in a Chlorocyclization Reaction: Concomitant Enantiomer Differentiation and Face Selective Alkene Chlorination by a Single Catalyst. *J. Am. Chem. Soc.* **2013**, *135*, 14806.

(20) Kitagawa, O.; Hanano, T.; Tanabe, K.; Shiro, M.; Taguchi, T. Enantioselective halocyclization reaction using a chiral titanium complex. *J. Chem. Soc.-Chem. Commun.* **1992**, 1005.

(21) Lee, H. J.; Kim, D. Y. Catalytic enantioselective bromolactonization of alkenoic acids in the presence of palladium complexes. *Tetrahedron Lett.* **2012**, *53*, 6984.

(22) Li, L.; Su, C.; Liu, X.; Tian, H.; Shi, Y. Catalytic Asymmetric Intermolecular Bromoesterification of Unfunctionalized Olefins. *Org. Lett.* **2014**, *16*, 3728.

(23) Lozano, O.; Blessley, G.; del Campo, T. M.; Thompson, A. L.; Giuffredi, G. T.; Bettati, M.; Walker, M.; Borman, R.; Gouverneur, V. Organocatalyzed Enantioselective Fluorocyclizations. *Angew. Chem. Int. Ed.* **2011**, *50*, 8105.

(24) Mizar, P.; Burrelli, A.; Gunther, E.; Softje, M.; Farooq, U.; Wirth, T. Organocatalytic Stereoselective Iodoamination of Alkenes. *Chem. Eur. J.* **2014**, *20*, 13113.

(25) Moyano, A.; Rios, R. Asymmetric Organocatalytic Cyclization and Cycloaddition Reactions. *Chem. Rev.* **2011**, *111*, 4703.

(26) Murai, K.; Fujioka, H. Recent progress in organocatalytic asymmetric halocyclization. *Heterocycles* **2013**, *87*, 763.

(27) Murai, K.; Matsushita, T.; Nakamura, A.; Fukushima, S.; Shimura, M.; Fujioka, H. Asymmetric Bromolactonization Catalyzed by a C(3)-Symmetric Chiral Trisimidazoline. *Angew. Chem. Int. Ed.* **2010**, *49*, 9174.

(28) Murai, K.; Nakamura, A.; Matsushita, T.; Shimura, M.; Fujioka, H. C3-Symmetric Trisimidazoline-Catalyzed Enantioselective Bromolactonization of Internal Alkenoic Acids. *Chem. Eur. J.* **2012**, *18*, 8448.

(29) Paull, D. H.; Fang, C.; Donald, J. R.; Pansick, A. D.; Martin, S. F. Bifunctional Catalyst Promotes Highly Enantioselective Bromolactonizations To Generate Stereogenic C-Br Bonds. *J. Am. Chem. Soc.* **2012**, *134*, 11128.

(30) Snider, B. B.; Johnston, M. I. Regioselectivity of the halolactonization of gamma,delta-unsaturated acids. *Tetrahedron Lett.* **1985**, *26*, 5497.

(31) Tan, C. K.; Le, C. C.; Yeung, Y. Y. Enantioselective bromolactonization of cis-1,2-disubstituted olefinic acids using an amino-thiocarbamate catalyst. *Chem. Commun.* **2012**, *48*, 5793.

(32) Tan, C. K.; Zhou, L.; Yeung, Y. Y. Organocatalytic Enantioselective Halolactonizations: Strategies of Halogen Activation. *Synlett* **2011**, 1335.

(33) Tan, C. K.; Zhou, L.; Yeung, Y. Y. Aminothiocarbamate-Catalyzed Asymmetric Bromolactonization of 1,2-Disubstituted Olefinic Acids. *Org. Lett.* **2011**, *13*, 2738.

(34) Tungen, J. E.; Nolsoe, J. M. J.; Hansen, T. V. Asymmetric Iodolactonization Utilizing Chiral Squaramides. *Org. Lett.* **2012**, *14*, 5884.

(35) Veitch, G. E.; Jacobsen, E. N. Tertiary Aminourea-Catalyzed Enantioselective Iodolactonization. *Angew. Chem. Int. Ed.* **2010**, *49*, 7332.

(36) Wang, M.; Gao, L. X.; Mai, W. P.; Xia, A. X.; Wang, F.; Zhang, S. B. Enantioselective iodolactonization catalyzed by chiral quaternary ammonium salts derived from cinchonidine. *J. Org. Chem.* **2004**, *69*, 2874.

(37) Wang, M.; Gao, L. X.; Yue, W.; Mai, W. P. Reagent-controlled asymmetric iodolactonization using cinchona alkaloids as chiral sources. *Synth. Commun.* **2004**, *34*, 1023.

(38) Wang, Y. M.; Wu, J.; Hoong, C.; Rauniyar, V.; Toste, F. D. Enantioselective Halocyclization Using Reagents Tailored for Chiral Anion Phase-Transfer Catalysis. *J. Am. Chem. Soc.* **2012**, *134*, 12928.

(39) Whitehead, D. C.; Fhaner, M.; Borhan, B. A peptide bromoiodinane approach for asymmetric bromolactonization. *Tetrahedron Lett.* **2011**, *52*, 2288.

(40) Whitehead, D. C.; Yousefi, R.; Jaganathan, A.; Borhan, B. An Organocatalytic Asymmetric Chlorolactonization. *J. Am. Chem. Soc.* **2010**, *132*, 3298.

(41) Yin, Q.; You, S.-L. Enantioselective Chlorocyclization of Indole Derived Benzamides for the Synthesis of Spiro-indolines. *Org. Lett.* **2013**, *15*, 4266.

(42) Yin, Q.; You, S.-L. Asymmetric Chlorocyclization of Indole-3-yl-benzamides for the Construction of Fused Indolines. *Org. Lett.* **2014**, *16*, 2426.

(43) Yin, Q.; You, S.-L. Asymmetric Chlorination/Ring Expansion for the Synthesis of α-Quaternary Cycloalkanones. *Org. Lett.* **2014**, *16*, 1810.

(44) Zhang, J. L.; Wang, J.; Qiu, Z. B.; Wang, Y. Highly regio- and diastereoselective halohydroxylation of olefins: a facile synthesis of vicinal halohydrins. *Tetrahedron* **2011**, *67*, 6859.

(45) Chen, J.; Zhou, L. Recent Progress in the Asymmetric Intermolecular Halogenation of Alkenes. *Synthesis-Stuttgart* **2014**, *46*, 586.

(46) Cheng, Y. A.; Yu, W. Z.; Yeung, Y. Y. Recent advances in asymmetric intra- and intermolecular halofunctionalizations of alkenes. *Org. Biomol. Chem.* **2014**, *12*, 2333.

(47) Chung, W. J.; Vanderwal, C. D. Stereoselective Halogenation in Natural Product Synthesis. *Angew. Chem. Int. Ed. Engl.* **2016**, *55*, 4396.

(48) Denmark, S. E.; Kuester, W. E.; Burk, M. T. Catalytic, Asymmetric Halofunctionalization of Alkenes-A Critical Perspective. *Angew. Chem. Int. Ed.* **2012**, *51*, 10938.

(49) Landry, M. L.; Burns, N. Z. Catalytic Enantioselective Dihalogenation in Total Synthesis. *Acc. Chem. Res.* **2018**, *51*, 1260.

(50) Tan, C. K.; Yeung, Y. Y. Recent advances in stereoselective bromofunctionalization of alkenes using N-bromoamide reagents. *Chem. Commun.* **2013**, *49*, 7985.

(51) Kolb, H. C.; Andersson, P. G.; Sharpless, K. B. Toward an understanding of the high enantioselectivity in the osmium-catalyzed asymmetric dihydroxylation. 1. Kinetics. *J. Am. Chem. Soc.* **1994**, *116*, 1278.

(52) Jaganathan, A.; Borhan, B. Chlorosulfonamide Salts Are Superior Electrophilic Chlorine Precursors for the Organocatalytic Asymmetric Chlorocyclization of Unsaturated Amides. *Org. Lett.* **2014**, *16*, 3616.

(53) Niu, W.; Yeung, Y.-Y. Catalytic and Highly Enantioselective Selenolactonization. *Org. Lett.* **2015**, *17*, 1660.

(54) Nicolaou, K. C.; Simmons, N. L.; Ying, Y.; Heretsch, P. M.; Chen, J. S. Enantioselective Dichlorination of Allylic Alcohols. *J. Am. Chem. Soc.* **2011**, *133*, 8134.

(55) Wilking, M.; Mück-Lichtenfeld, C.; Daniliuc, C. G.; Hennecke, U. Enantioselective, Desymmetrizing Bromolactonization of Alkynes. *J. Am. Chem. Soc.* **2013**, *135*, 8133.

(56) Yousefi, R.; Ashtekar, K. D.; Whitehead, D. C.; Jackson, J. E.; Borhan, B. Dissecting the Stereocontrol Elements of a Catalytic Asymmetric Chlorolactonization: Syn Addition Obviates Bridging Chloronium. *J. Am. Chem. Soc.* **2013**, *135*, 14524.

(57) Yousefi, R.; Whitehead, D. C.; Mueller, J. M.; Staples, R. J.; Borhan, B. On the Chlorenium Source in the Asymmetric Chlorolactonization Reaction. *Org. Lett.* **2011**, *13*, 608.

(58) Ashtekar, K. D.; Marzijarani, N. S.; Jaganathan, A.; Holmes, D.; Jackson, J. E.; Borhan, B. A New Tool To Guide Halofunctionalization Reactions: The Halenium Affinity (*HalA*) Scale. *J. Am. Chem. Soc.* **2014**, *136*, 13355.

(59) Blackmond, D. G. Reaction progress kinetic analysis: A powerful methodology for mechanistic studies of complex catalytic reactions. *Angew. Chem. Int. Ed.* **2005**, *44*, 4302.

(60) Mathew, J. S.; Klussmann, M.; Iwamura, H.; Valera, F.; Futran, A.; Emanuelsson, E. A. C.; Blackmond, D. G. Investigations of Pd-catalyzed ArX coupling reactions informed by reaction progress kinetic analysis. *J. Org. Chem.* **2006**, *71*, 4711.

(61) Blackmond, D. G. Kinetic Profiling of Catalytic Organic Reactions as a Mechanistic Tool. *J. Am. Chem. Soc.* **2015**, *137*, 10852.

(62) Nielsen, C. D.; Bures, J. Visual kinetic analysis. *Chem. Sci.* **2019**, *10*, 348.

(63) Ashtekar, K. D.; Vetticatt, M.; Yousefi, R.; Jackson, J. E.; Borhan, B. Nucleophile-Assisted Alkene Activation: Olefins Alone Are Often Incompetent. *J. Am. Chem. Soc.* **2016**, *138*, 8114.

(64) Burgi, T.; Baiker, A. Conformational behavior of cinchonidine in different solvents: A combined NMR and ab initio investigation. *J. Am. Chem. Soc.* **1998**, *120*, 12920.

(65) Dijkstra, G. D. H.; Kellogg, R. M.; Wynberg, H. Conformational study of cinchona alkaloids - A combined NMR and molecular-orbital approach. *J. Org. Chem.* **1990**, *55*, 6121.

(66) Olsen, R. A.; Borchardt, D.; Mink, L.; Agarwal, A.; Mueller, L. J.; Zaera, F. Effect of protonation on the conformation of cinchonidine. *J. Am. Chem. Soc.* **2006**, *128*, 15594.

(67) Ammalahti, E.; Bardet, M.; Cadet, J.; Molko, D. NMR assignments and conformational studies of two diastereomeric oxidation products of 2 '-deoxycytidine. *Magn. Reson. Chem.* **1998**, *36*, 363.

(68) Ammalahti, E.; Bardet, M.; Molko, D.; Cadet, J. Evaluation of distances from ROESY experiments with the intensity-ratio method. *J. Magn. Reson. A.* **1996**, *122*, 230.

(69) Bodenhausen, G.; Ernst, R. R. Direct Determination of Rate Constants of Slow Dynamic Processes by Two-Dimensional Accordion Spectroscopy in Nuclear Magnetic-Resonance. *J. Am. Chem. Soc.* **1982**, *104*, 1304.

Insert Table of Contents artwork here